

On the synchronization of spatially coupled oscillators

Angelo Cenedese, Chiara Favaretto

Abstract—Over the past decade, considerable attention has been devoted to the problem of emergence of synchronization patterns in a network of coupled oscillators, which can be observed in a variety of disciplines, from the biological to the engineering fields. In this context, the Kuramoto model is a classical model for describing synchronization phenomena that arise in large-scale systems that exploit local information and interactions. In this work, an extension of such a model is presented, that considers the spatial distances among the oscillator nodes. In detail, coupling strength and spatial conditions are derived, needed to reach phase cohesiveness and frequency synchronization, both in the scenario when a single population of agents is present and when two different populations interact. These theoretical findings are confirmed by extensive numerical Monte Carlo simulations and statistical analysis.

I. INTRODUCTION

Over the past decades, a considerable attention has been devoted to the problem of the coordinated motion of multiple autonomous agents. In a variety of disciplines, researchers have been developing an understanding of how a group of moving objects can reach a consensus and move information without centralized coordination [18], [14], [17]. In this paper, we consider the synchronization of coupled nonlinear oscillators in networked systems, which finds its motivation in the study of a wide range of applications spanning from large scale systems in nature (e.g. brain dynamics [7], [15], cardiac pacemakers [8]) to human-related artificial networks (e.g. collective swarm motion [13], smart grids [6]).

In this context, a classical and very popular model to address the synchronization of coupled oscillators is the Kuramoto model that has been extensively studied from the seminal paper [10] to more recent works [16], [1], [4] (just to cite a few). In this simple model, a set of $N \geq 2$ coupled oscillators is considered, each characterized by a phase $\theta_i(t) \in \mathbb{T}^1$ (model state) and a natural frequency $\omega_i \in \mathbb{R}$ (model parameter), obeying to the following dynamics:

$$\dot{\theta}_i(t) = \omega_i - \frac{K}{N} \sum_{j=1}^N \sin(\theta_i(t) - \theta_j(t)), \quad i=1, \dots, N \quad (1)$$

where $K > 0$ is the coupling strength among the oscillators. Here, only the temporal behavior of the agent states is considered and (1) does not include any information related to the spatial configuration of the oscillators' network.

A. Cenedese and C. Favaretto are with the Department of Information Engineering, University of Padova, via Gradenigo 6/B, 35131 Padova, Italy. Corresponding author: A. Cenedese, angelo.cenedese@unipd.it.

This technical report is an extended version of the work presented at the Conference on Decision and Control 2015 (CDC15). In case of citation, please cite the CDC paper (same authors and title).

However, from an application point of view, it appears useful to understand how the spatial displacement of the oscillators affects their mutual coupling since, intuitively, the influence between two nodes will diminish with increasing their distance.

For example, the authors of [2] state that a crucial step toward neurobiological plausibility of coupled oscillators is the incorporation of time delay effects linked to a spatial metric. The dynamics of such a model introduces connection strengths that vary with distance and global connectivity is achieved by combining time delay effects with a finite width spatial kernel $W(i, j)$. Similarly, the importance of spatial displacement and time delay effects in biological oscillators network appears also in [3], which deals with the brain's neural activity on a network of N nodes, to study the structural connectivity in the brain in terms of connection strengths and conduction delays. Interestingly, analogous considerations regard also the study of the electric power grid dynamics where, again, the Kuramoto model proves to be an agile and useful model tool. In particular, [11] describes a spatially embedded Kuramoto dynamics that involves a constant delay proportional to the spatial distance between the oscillators, phase shifts caused by transmission delays and a coupling function that decreases with the distance. More in general, the basic idea that the distances among the agents affect the synchronization dynamics can be found also in [9], where it is considered the behavior of a lattice of oscillators that interact with a power-law coupling strength.

Given these premises and driven by interest both in biology and in power networks, in this paper a method is studied to embed the spatial component in the classic Kuramoto model (1), which considers the oscillators as located on a plane (as often occurs in real world applications), and introduces a kernel function $W(i, j)$ that (inversely) depends on the Euclidean distance among the oscillators. Differently from [2], such a kernel function smoothly decreases with the distance, while remaining always positive. Furthermore, sufficient conditions on the nominal $K > 0$ coupling strength and on the largest distance α_{max} are obtained, which permit to achieve *frequency synchronization* and *phase cohesiveness* (defined in Sec. III). More specifically, this work takes into account also the case in which the oscillators are influenced by different kernels, depending on their displacement in a specific area: in such a situation, the synchronization frequency changes if compared to the case where a single kernel characterizes the oscillator population.

The remainder of this paper is organized as follows. In Sec. II the modified Kuramoto model is proposed and in

Sec. III the main results are presented: firstly, sufficient explicit conditions for phase cohesiveness and frequency synchronization are established (Props. 1-2), and, then, the employment of two different kernels is studied (Prop. 3). Sec. IV presents some numerical simulations to validate and assess the theoretical findings and also statistical results are reported. Finally, Sec. V draws some final observations and gives insight into future developments.

II. SPATIALLY COUPLED OSCILLATORS NETWORK

In this work we consider a system of N coupled oscillators, distributed on a surface and represented by a graph. A graph $\mathcal{G} = (\mathcal{V}, \mathcal{E})$ is composed of a set of nodes, $\mathcal{V} = \{1, \dots, N\}$, consisting of the indices of the N agents of the network, and of a set of edges $\mathcal{E} \subseteq \mathcal{V} \times \mathcal{V}$, in which each edge connects one node to another (see for example, [12]). The edge (j, i) indicates that agent j can transmit information to agent i . If there is a directed path from node j to i , then node i is said to be reachable from node j . If each node is reachable from all the others, then \mathcal{G} is said to be *strongly connected*. Moreover, the graph is said to be *fully connected* if there exists an edge connecting each pairs of nodes. In this paper, we consider fully connected graphs.

Given this framework, each oscillator node i is characterized by its (static) spatial coordinates $(x_i, y_i) \in \mathbb{R}^2$ and is endowed with a state that is its phase angle $\theta_i(t) \in \mathbb{T}^1$ (\mathbb{T}^1 is the one dimensional torus set, i.e. the set $[0, 2\pi]$ where 0 corresponds to 2π), which obeys the dynamics

$$\dot{\theta}_i(t) = \omega_i - \frac{K}{N} \sum_{j=1}^N W(i, j) \sin(\theta_i(t) - \theta_j(t)), \quad (2)$$

where $\omega_i \in \mathbb{R}$ is the oscillator natural frequency (namely: the dynamics of each isolated node is $\dot{\theta}_i(t) = \omega_i$), $K \in \mathbb{R}$ is the maximum coupling strength among the oscillators, and $W(i, j) \in]0, 1]$ is a kernel function that depends on the Euclidean distance α_{ij} among the agents, as follows:

$$W(i, j) = \exp\left(-\left(\frac{\alpha_{ij}}{p}\right)^2\right),$$

where p is a kernel shaping parameter.

In summary, the dynamics (2) represents a modified Kuramoto model that considers also the spatial displacements of the oscillator nodes, while the interaction topology among such oscillators is modeled by \mathcal{G} and weighed by the state-independent and time-invariant kernel function W .

III. SYNCHRONIZATION PROBLEM AND BOUNDS

When analyzing the behavior of the oscillators network (2), different kinds of synchronization can be considered [5]:

- *Frequency synchronization*: all frequencies $\{\dot{\theta}_i(t)\}$ converge to a common constant frequency $\omega_{sync} \in \mathbb{R}$ as $t \rightarrow \infty$, where $\omega_{sync} = \frac{1}{N} \sum_{i=1}^N \omega_i$; if the vector of the natural frequencies is in the orthogonal complement of the ones vector, $[\omega_1, \dots, \omega_N]^\top \in \mathbf{1}_N^\perp$, then $\omega_{sync} = 0^1$.

¹According to [5], this assumption is not limiting the study since all frequencies expressed w.r.t. ω_{sync} as $\omega_i - \omega_{sync}$ in a rotating frame.

- *Phase synchronization*: all phases $\{\theta_i(t)\}$ becomes identical as $t \rightarrow \infty$; this state can be reached only if all natural frequencies $\{\omega_i\}$ are identical.

In the case when phase synchronization cannot be achieved:

- *Phase cohesiveness*: for $\gamma \in [0, \pi[$, let $\overline{\Delta}_{\mathcal{G}}(\gamma) \in \mathbb{T}^N$ be the closed set of angle arrays $(\theta_1, \dots, \theta_N)$ s.t. $|\theta_i - \theta_j| \leq \gamma, \forall (i, j) \in \mathcal{E}$. Note that if $\gamma = 0$ this is tantamount phase synchronization ($\Delta_{\mathcal{G}}(\gamma)$ is the interior of $\overline{\Delta}_{\mathcal{G}}(\gamma)$).
- *Arc invariance*: for $\gamma \in [0, 2\pi[$, let $\overline{Arc}_N(\gamma) \in \mathbb{T}^N$ be the closed set of angle arrays $\theta = (\theta_1, \dots, \theta_N)$ s.t. there exists an arc of length γ containing all $\theta_1, \dots, \theta_N$. It means that $\theta \in \overline{Arc}_N(\gamma)$ satisfies $\max_{i, j \in \{1, \dots, N\}} |\theta_i - \theta_j| \leq \gamma$ ($Arc_N(\gamma)$ is the interior of $\overline{Arc}_N(\gamma)$).

This study focuses on frequency synchronization and phase cohesiveness, with phase distances $|\theta_i - \theta_j|$ limited by $\gamma < \pi/2$, which is of interest and utility for most applications.

A useful metric to analyze the level of the system synchronization is the order parameter, introduced in [10] as

$$\rho e^{j\phi} = \frac{1}{N} \sum_{i=1}^N e^{j\theta_i}, \quad (3)$$

which represents the centroid of all the phases of the oscillators, when these are seen as points on the unit circle in \mathbb{S}^1 . The magnitude $\rho \in [0, 1]$ is a synchronization measure: if all oscillators are phase synchronized, then $\rho = 1$, whereas if they are balanced (i.e. uniformly distributed over the unit circle), then $\rho = 0$. In particular, it is useful to recall the following Lemma [5, Lemma 3.1].

Lemma 1: Shortest Arc Length and Order Parameter

Consider an array of $N \geq 2$ angles $\theta = (\theta_1, \dots, \theta_N) \in \mathbb{T}^N$ and compute the magnitude $\rho(\theta) = \frac{1}{N} \left| \sum_{i=1}^N e^{j\theta_i} \right|$. Let $\gamma(\theta)$ be the length of the shortest arc containing all angles, that is, $\theta \in \overline{Arc}_N(\gamma(\theta))$. The following statements holds:

- 1) if $\gamma(\theta) \in [0, \pi]$, then $\rho(\theta) \in [\cos(\gamma(\theta)/2), 1]$;
- 2) if $\theta \in \overline{Arc}_N(\pi)$, then $\gamma(\theta) \in [2 \arccos(\rho(\theta)), \pi]$.

A. Single Kernel Convergence Bounds

Following the results summarized in [5], the interest is now to establish some explicit conditions for the modified Kuramoto model (2). In doing so, the following propositions extend the results in [4], involving the coupling strength parameter K and the maximum α_{max} of the Euclidean distances $\{\alpha_{ij}\}$ between the oscillators, to achieve a synchronized state for θ , namely a state where frequency synchronization and phase cohesiveness coexist.

Proposition 1: Phase cohesiveness

Consider the Kuramoto model (2), with $N \geq 2$ oscillators, natural frequencies $\omega \in \mathbf{1}_N^\perp$ in $[\omega_{min}, \omega_{max}]$ and coupling strength K . If the coupling strength K is higher than a critical value K_{cr} :

$$K > K_{cr} = \frac{\omega_{max} - \omega_{min}}{e^{-\tilde{\alpha}^2}} \quad \text{with} \quad \tilde{\alpha} = \frac{\alpha_{max}}{p} \quad (4)$$

then $\exists \gamma_{max} \in]\pi/2, \pi]$ and $\exists \gamma_{min} \in [0, \pi/2[$ such that

- 1) $\overline{Arc}_N(\gamma)$ is positively invariant for every $\gamma \in [\gamma_{min}, \gamma_{max}]$ and each trajectory originating in $Arc_N(\gamma_{max})$ approaches asymptotically $\overline{Arc}_N(\gamma_{min})$ (phase cohesiveness);
- 2) $\sin(\gamma_{min}) = \sin(\gamma_{max}) = K_{cr}/K$.

Remark 1: Interestingly, in this framework, a dependence between the coupling strength K and the maximum distance α_{max} among agents can be stated. Indeed, relation (4) is equivalent to the following condition:

$$\alpha_{max} < \alpha_{cr} = p \sqrt{-\ln \left(\frac{\omega_{max} - \omega_{min}}{K} \right)}. \quad (5)$$

In practice, if a model (2) is given, with an imposed spatial distribution $\{\alpha_{ij} \leq \alpha_{max}\}$, to achieve phase cohesiveness there must be exerted a coupling strength larger than K_{cr} . Conversely, if the network interactions are bounded by some coupling strength value K , the displacement among the agent should also be bounded (by α_{cr}) in order to achieve synchronization.

It is worth noticing that α_{cr} shows a linear dependence on the kernel parameter p ; moreover, the upper bound for α_{max} is really restrictive for a low value of p and remains low also increasing K .

Proposition 2: Frequency synchronization

With a coupling strength $K > K_{cr}$, model (2) achieves exponential frequency synchronization for all possible distributions of the natural frequencies $\{\omega_i\}$ on the compact interval $[\omega_{min}, \omega_{max}]$ and for all initial phase conditions $\theta_i(0) \in Arc_N(\gamma_{max})$. Moreover:

- 1) the asymptotic synchronization frequency ω_{sync} is the average frequency $\omega_{avg} = \frac{1}{N} \sum_{i=1}^N \omega_i$;
- 2) given phase cohesiveness in $\Delta(\gamma)$ for some fixed $\gamma < \pi/2$, the exponential synchronization rate is no worse than $\lambda_{fs} = K e^{-\alpha^2} \cos(\gamma)$;

The proofs of Props.1 and 2 develop along the same line as that of [4, Theorem 4.1], by introducing a Lyapunov function $V: \mathbb{T}^N \rightarrow [0, \pi]$ that measures the convergence trend, as

$$V(\theta) = \max \{|\theta_i - \theta_j| \text{ s.t. } i, j \in \{1, \dots, N\}\}.$$

For completeness, they are reported in App. I.

Corollary 1: Consider model (2) in the conditions stated by Prop. 1: the asymptotic value ρ_∞ of the magnitude of the order parameter (3) is bounded as

$$1 \geq \rho_\infty \geq \cos \left(\frac{\gamma_{min}}{2} \right) = \sqrt{\frac{1 + \sqrt{1 - \left(\frac{\omega_{max} - \omega_{min}}{K e^{-\alpha^2}} \right)^2}}{2}}. \quad (6)$$

Proof: As a consequence of 1) of Prop. 1 and Lemma 1, the asymptotic magnitude of the order parameter obeys

$$1 \geq \rho_\infty \geq \cos \left(\frac{\gamma_{min}}{2} \right) = \sqrt{\frac{1 + \cos(\gamma_{min})}{2}} := \rho_{\infty, min}. \quad (7)$$

From 2) of Prop. 1, it follows

$$\cos(\gamma_{min}) = \sqrt{1 - \left(\frac{\omega_{max} - \omega_{min}}{K e^{-\alpha^2}} \right)^2}, \quad (8)$$

and from (8) and (7), (6) is proved. ■

B. Two Kernel Configuration

It is now interesting to move to the case in which two populations of agents with different kernels interact.

For this purpose, a configuration is considered as composed by two different regions, populated by sets \mathcal{A}_m and \mathcal{A}_M that are characterized respectively by two different kernels $W_m(i, j)$ and $W_M(i, j)$, related to parameters $p_m < p_M$. For the time being, the cardinality of the two populations is the same: $N/2$ oscillators belong to \mathcal{A}_m and the others $N/2$ to \mathcal{A}_M . The system dynamics becomes:

$$\dot{\theta}_i(t) = \omega_i - \frac{K}{N} \begin{cases} \sum W_m(i, j) \sin(\theta_i(t) - \theta_j(t)), & i \in \mathcal{A}_m \\ \sum W_M(i, j) \sin(\theta_i(t) - \theta_j(t)), & i \in \mathcal{A}_M \end{cases}$$

where

$$W_m(i, j) = e^{-\left(\frac{\alpha_{i,j}}{p_m}\right)^2} < e^{-\left(\frac{\alpha_{i,j}}{p_M}\right)^2} = W_M(i, j),$$

which yields:

$$K_{cr} = \frac{\omega_{max} - \omega_{min}}{e^{-\left(\frac{\alpha_{max}}{p_m}\right)^2}}.$$

Unlike the single kernel case, where $\omega_{sync} = \frac{1}{N} \sum_{i=1}^N \omega_i = 0$, in the two kernels case the following lemma stands:

Lemma 2: Synchronization frequency with two kernels

Consider a system of an even numbers $N \geq 2$ of oscillators, characterized by their spatial coordinates (x_i, y_i) and their phases $\theta_i(t)$. Let $\omega \in \mathbf{1}_N^{\frac{1}{N}}$ be the vector of the natural frequencies. If K and α_{max} are such that there is frequency synchronization among the oscillators, then, the synchronization frequency $\tilde{\omega}_{sync}$ results, for $t \gg 0$:

$$\tilde{\omega}_{sync} = \frac{K}{N^2} \sum_{\substack{i \in \mathcal{A}_m \\ j \in \mathcal{A}_M}} (W_M(j, i) - W_m(i, j)) \sin(\theta_i - \theta_j).$$

Proof: By summing over all nodes it follows:

$$\begin{aligned} \sum_{i=1}^N \dot{\theta}_i &= \sum_{i=1}^N \omega_i - \frac{K}{N} \sum_{i \in \mathcal{A}_m} \sum_{j=1}^N W_m(i, j) \sin(\theta_i - \theta_j) + \\ &\quad - \frac{K}{N} \sum_{i \in \mathcal{A}_M} \sum_{j=1}^N W_M(i, j) \sin(\theta_i - \theta_j). \end{aligned} \quad (9)$$

By noticing that if $i, j \in \mathcal{A}_*$ then $W_*(i, j) = W_*(j, i)$ (* being equal to m or M) and $\sin(\theta_i - \theta_j) = -\sin(\theta_j - \theta_i)$, after some calculation (9) simplifies to

$$\sum_{i=1}^N \dot{\theta}_i = \sum_{i=1}^N \omega_i - \frac{K}{N} \sum_{\substack{i \in \mathcal{A}_m \\ j \in \mathcal{A}_M}} (W_m(i, j) - W_M(j, i)) \sin(\theta_i - \theta_j).$$

Hence, normalizing by the network cardinality N , it follows:

$$\begin{aligned} \tilde{\omega}_{sync} &= \frac{1}{N} \sum_{i=1}^N \dot{\theta}_i \\ &= \omega_{sync} + \frac{K}{N^2} \sum_{\substack{i \in \mathcal{A}_m \\ j \in \mathcal{A}_M}} \underbrace{(W_M(j, i) - W_m(i, j)) \sin(\theta_i - \theta_j)}_{B(i, j)} \end{aligned} \quad (10)$$

which proves the thesis by recalling that $\omega_{sync} = 0$. ■

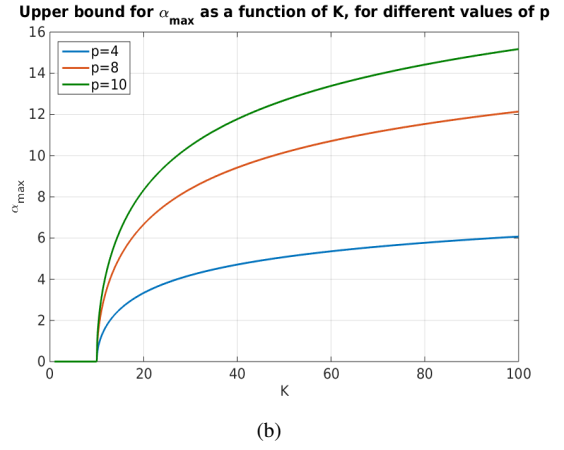
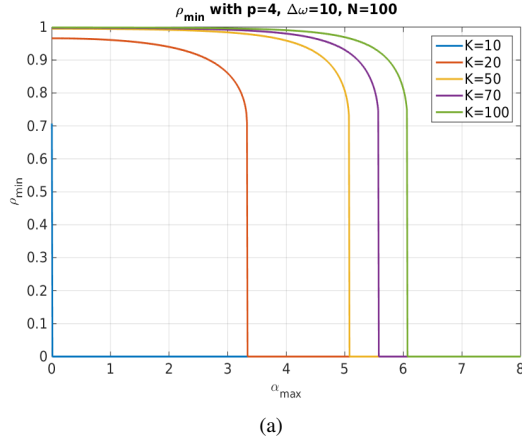


Fig. 1. (a) $\rho_{\infty, \min}$ as a function of α_{\max} with $p = 4$ (for different values of K); (b) Upper bound for α_{\max} as a function of K (for different values of p).

Namely, if the oscillator network can be described by two populations characterized by different spatial kernels, the synchronization frequency $\tilde{\omega}_{sync}$ deviates from the null average of the natural frequencies. This difference can be bounded w.r.t. the two kernels parameters as follows:

Proposition 3: Frequency Bound with Two Kernels

In the hypothesis of Lemma 2, a bound $\Delta\omega_M$ for the difference between the synchronization frequency $\tilde{\omega}_{sync}$ and $\omega_{sync} = 0$ is given by:

$$|\Delta\omega_{sync}| \leq \frac{K}{4} \left[e^{-\left(\frac{\alpha^*}{p_M}\right)^2} - e^{-\left(\frac{\alpha^*}{p_m}\right)^2} \right] = \Delta\omega_M, \quad (11)$$

where

$$\alpha^* = p_m p_M \sqrt{\frac{2}{p_M^2 - p_m^2} \ln\left(\frac{p_M}{p_m}\right)}.$$

Proof: From (10), $\Delta\omega_{sync} = \tilde{\omega}_{sync} - \omega_{sync}$ results as

$$\Delta\omega_{sync} = \frac{K}{N^2} \sum_{\substack{i \in \mathcal{A}_1 \\ j \in \mathcal{A}_M}} B(i, j), \quad (12)$$

and

$$\Delta W(i, j) = W_M(j, i) - W_m(i, j) = e^{-\left(\frac{\alpha_{i,j}}{p_M}\right)^2} - e^{-\left(\frac{\alpha_{i,j}}{p_m}\right)^2},$$

considering that $\alpha_{i,j} = \alpha_{j,i}$, $\forall i, j$.

To find its maximum value, the derivative is obtained:

$$\frac{\partial \Delta W}{\partial \alpha_{i,j}} = 2\alpha_{i,j} \left[\frac{1}{p_m^2} e^{-\left(\frac{\alpha_{i,j}}{p_m}\right)^2} - \frac{1}{p_M^2} e^{-\left(\frac{\alpha_{i,j}}{p_M}\right)^2} \right],$$

which becomes zero at $\alpha_{i,j} = 0$ (trivial minimum solution) and when

$$\alpha_{i,j} = \alpha^* = p_m p_M \sqrt{\frac{2}{p_M^2 - p_m^2} \ln\left(\frac{p_M}{p_m}\right)}.$$

As a consequence:

$$\Delta W \in \left[0, e^{-\left(\frac{\alpha^*}{p_M}\right)^2} - e^{-\left(\frac{\alpha^*}{p_m}\right)^2} \right],$$

and it follows that the absolute value of the quantity $B(i, j)$ highlighted in (12) is bounded in $\left[0, e^{-\left(\frac{\alpha^*}{p_M}\right)^2} - e^{-\left(\frac{\alpha^*}{p_m}\right)^2} \right]$.

As a consequence

$$\begin{aligned} |\Delta\omega_{sync}| &\leq \frac{K}{N^2} \sum_{\substack{i \in \mathcal{A}_1 \\ j \in \mathcal{A}_2}} \left[e^{-\left(\frac{\alpha^*}{p_M}\right)^2} - e^{-\left(\frac{\alpha^*}{p_m}\right)^2} \right] \quad (13) \\ &\leq \frac{K}{4} \left[e^{-\left(\frac{\alpha^*}{p_M}\right)^2} - e^{-\left(\frac{\alpha^*}{p_m}\right)^2} \right]. \end{aligned}$$

So far the case of two balanced populations of agents has been considered and indeed the bound (11) does not depend on the cardinality of the sets. Conversely, if the two kernels refer to uneven groups of oscillators, the results of Prop. 3 can be extended.

Be the sets \mathcal{A}_m and \mathcal{A}_M of different cardinalities, namely $|\mathcal{A}_m| = N_m$ and $|\mathcal{A}_M| = N_M = N - N_m$. In such conditions, relation (11) modifies to:

$$|\Delta\omega_{sync}| \leq K \frac{N_m (N - N_m)}{N^2} \left[e^{-\left(\frac{\alpha^*}{p_M}\right)^2} - e^{-\left(\frac{\alpha^*}{p_m}\right)^2} \right] \quad (14)$$

and the r.h.s. of (14) is a bound $\Delta\omega_M$ for $\Delta\omega_{sync}$. Its derivative w.r.t. N_m ,

$$\frac{\partial \Delta\omega_M}{\partial N_m} = K \left(\frac{N - 2N_m}{N^2} \right) \left[e^{-\left(\frac{\alpha^*}{p_M}\right)^2} - e^{-\left(\frac{\alpha^*}{p_m}\right)^2} \right],$$

equalizes to zero only at $N_m = N/2$ (point of maximum); also, the minimum value for the r.h.s. of (14) is achieved at the extreme points, i.e. when the two populations are strongly unbalanced:

$$\begin{cases} N_m = 1 \\ N_M = N - 1 \end{cases} \quad \text{or} \quad \begin{cases} N_m = N - 1 \\ N_M = 1 \end{cases}$$

In Fig. 2, an example of the trend of $\Delta\omega_M$ as a function of N_m is given with $K = 50$, $p_m = 3$ and $N = 50$, for different values of p_M .

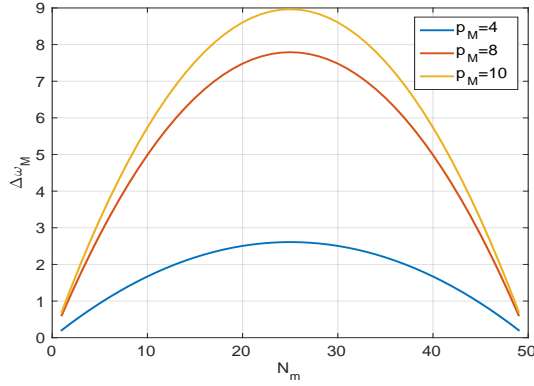


Fig. 2. Trend of $\Delta\omega_M$ as a function of N_m with $K = 50$, $p_m = 3$ and $N = 50$, for different values of p_M .

IV. NUMERICAL RESULTS

In this section, some simulations are presented to assess and validate the previously discussed theoretical findings.

Specifically, approximately $n = 30000$ Monte Carlo realizations have been generated for a random network of oscillators spatially placed on a spherical domain (in order to avoid edge effects) and considering geodesic distances among pairs of nodes. The number of agents N is sampled from a uniform distribution $\mathcal{U}([10, 200])$ and the radius of the spherical domain is $r \sim \mathcal{U}([0, 10])$; the network node position (x_i, y_i, z_i) is obtained as

$$\begin{cases} x_i = r \sin(\psi_i) \cos(\zeta_i) \\ y_i = r \sin(\psi_i) \sin(\zeta_i) \\ z_i = r \cos(\psi_i) \end{cases}$$

as a function of the two angles $\psi_i, \zeta_i \sim \mathcal{U}([0, 2\pi])$. Also, the maximum arc-distance among all nodes α_{max} can be calculated. As for the natural frequency distribution, for a given $N \geq 10$, the frequency vector $\omega \in \mathbf{1}_N^{\perp}$ is constructed in two steps. Firstly, N real numbers q_i are sampled from $\mathcal{U}([-1, +1])$; then, by subtracting the average $\frac{1}{N} \sum_{i=1}^N q_i$, $\omega_i = q_i - \frac{1}{N} \sum_{i=1}^N q_i$ is defined to obtain $\omega = (\omega_1, \dots, \omega_N)^T \in \mathbf{1}_N^{\perp}$. Finally, a random parameter $p \in \{1, 2, \dots, 10\}$ and a random $\gamma_{max} \in]\pi/2, \pi]$ are chosen; $\gamma_{min} \in [0, \pi/2[$ is selected such that $\sin(\gamma_{max}) = \sin(\gamma_{min})$. Hence, a set of N oscillators $\theta_i(0)$ is generated, with $\theta(0) \in \text{Arc}_N(\gamma_{max})$. The bound gain is defined as $K_{cr} = \frac{\Delta\omega}{e_{-\left(\frac{\alpha_{max}}{p}\right)^2}}$, and the coupling strength K to ensure synchronization is obtained:

$$K = \frac{K_{cr}}{\sin(\gamma_{max})} > K_{cr}.$$

In Fig. 3 two examples are shown. The top row refers to (a) the single kernel case, where (b) phase cohesiveness is reached and (c) the Lyapunov function $V(\theta(t))$ behaves according to Prop. 1; the bottom row, instead, is related to (d) a two kernel configuration, where (e) phase cohesiveness is attained for the two populations and (f) the frequency convergence is bounded by (14).

More in general, the assessment of the correctness and the accuracy of Prop. 1 for arbitrary networks is carried out by solving (2) for each instance and testing the assumptions:

$$\begin{aligned} \mathcal{H}_{fr} : & \begin{cases} \gamma_{max} \in]\pi/2, \pi] \\ K = \frac{K_{cr}}{\sin(\gamma_{max})} > K_{cr} \end{cases} \Rightarrow \dot{\theta} \xrightarrow[t \rightarrow \infty]{} \omega_{sync} \mathbf{1}_N \\ \mathcal{H}_{ph} : & \begin{cases} \gamma_{max} \in]\pi/2, \pi] \\ K = \frac{K_{cr}}{\sin(\gamma_{max})} > K_{cr} \end{cases} \Rightarrow \theta(T) \in \overline{\text{Arc}_N}(\gamma_{min}) \end{aligned}$$

In this context, frequency synchronization is achieved if the differences among the mean values of the last 50 samples of the frequencies $\bar{\theta}_i$ remain below a threshold $\epsilon_f = 10^{-2}$, i.e.

$$|\bar{\theta}_i - \bar{\theta}_j| < \epsilon_f, \quad \forall i, j \in \{1, \dots, N\};$$

phase cohesiveness is reached at the simulation time T if

$$|\theta_i(T) - \theta_j(T)| \leq \gamma_{min}, \quad \forall i, j \in \{1, \dots, N\}.$$

The empirical probability $\hat{\mathcal{P}}$ for hypotheses \mathcal{H}_* (\mathcal{H}_* being \mathcal{H}_{fr} or \mathcal{H}_{ph}) is computed and, to obtain an accuracy level of $\epsilon = 0.01$ and a confidence level of $\eta = 0.01$,

$$\mathcal{P} \left(\left| \mathcal{P}(\mathcal{H}_* \text{ is true}) - \hat{\mathcal{P}}(\mathcal{H}_* \text{ is true}) \right| < \epsilon \right) > 1 - \eta,$$

the Chernoff-Hoeffding bound justifies the chosen number of nominal models n

$$n \geq \frac{1}{2\epsilon^2} \ln \frac{2}{\eta} = 26492.$$

In particular, the Monte Carlo simulations in the theoretical cohesiveness and synchronization conditions stated before show that

$$\hat{\mathcal{P}}_{fr} = 88.26\% \quad \hat{\mathcal{P}}_{ph} = 100\%. \quad (15)$$

Indeed, while the value of $\hat{\mathcal{P}}_{ph}$ is really satisfactory, i.e. phase cohesiveness is always obtained, the low value of $\hat{\mathcal{P}}_{fr}$ is probably due to the threshold-based method adopted for assessing frequency synchronization and to the high values of K (sometimes much higher than necessary) that may lead to numerical issues, as it will be clearer later.

In this respect, it is interesting to study the bound accuracy, i.e. to find the smallest value K_{min} that permits to achieve phase cohesiveness in $\overline{\Delta}(\gamma_{min})$. For each sample network out of n Monte Carlo realizations, the smallest value of K leading to cohesive phases satisfying $|\max |\theta_i - \theta_j| - \gamma_{min}| < \epsilon_{ph}$, where $\epsilon_{ph} = 0.5^\circ$, is found iteratively by numerically integrating the dynamics (2): at the h -th iteration the following scheme is applied:

- if $|\max |\theta_i - \theta_j| - \gamma_{min}| < \epsilon_{ph}$ then $K^{(h)} = K_{min}$;
- if $\max |\theta_i - \theta_j| < \gamma_{min} - \epsilon_{ph}$ then $K^{(h+1)} = 0.9K^{(h)}$;
- if $\max |\theta_i - \theta_j| > \gamma_{min} + \epsilon_{ph}$ then $K^{(h+1)} = 1.1K^{(h)}$.

This iterative process stops when K_{min} is found or when the iterations exceed 1000.

By calling $K^{(1)} = K_{cr}/\sin(\gamma_{min})$, it is expected that the ratio $K_{min}/K^{(1)}$ is always lower than or equal to unity. Moreover, if that happens, it means that the value of K_{cr} is sufficient to achieve phase cohesiveness.

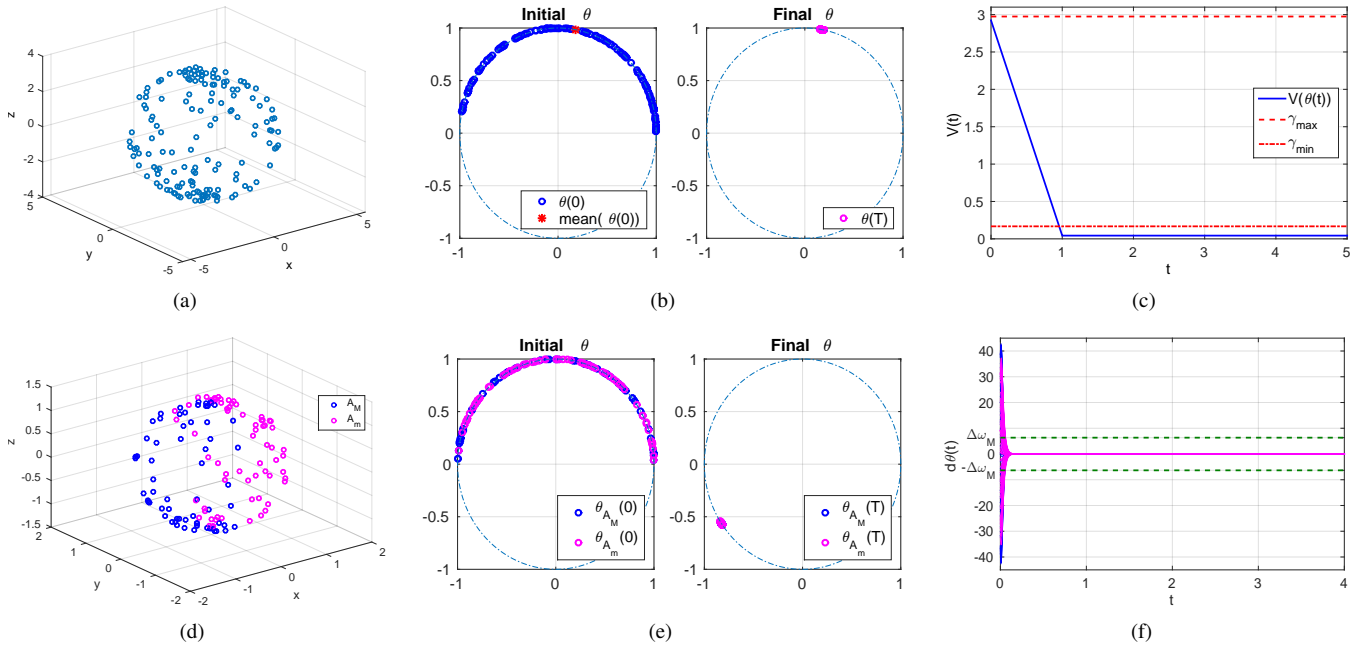


Fig. 3. Sample realizations of a single kernel (top row) and a two kernel (bottom row) oscillator network. *Single kernel network.* Parameters: $N = 153$, $r = 3.48$, $p = 8$, $\gamma_{max} = 170.4^\circ - \gamma_{min} = 9.6^\circ$, $K_{cr} = 12.47 - K = 74.89$. From left to right: spatial configuration of the agents, comparison between initial and final phases in the unit-circle, trend of the Lyapunov function $V(\theta(t))$. *Two kernel network.* Parameters: $N = 134$ ($N_M = 65 - N_m = 69$), $r = 1.34$, $p_M = 7 - p_m = 4$, $\gamma_{max} = 174.8^\circ - \gamma_{min} = 5.2^\circ$, $K_{cr} = 5.85 - K = 64.89$, $\Delta\omega_M = 6.3445 - \omega_{sync} = 0.0022$. From left to right: spatial configuration of the agents, comparison between initial and final phases in the unit-circle, trend of the oscillators' frequencies.

In Fig. 4, the statistical distribution of this ratio is shown: firstly, it can be observed that the probability of reaching phase cohesiveness as the percent number of samples with the ratio lower or equal to 1 is $\widehat{P}_{ph} = 100\%$.

Furthermore, by analyzing the statistical distribution, there is a certain set of sample simulations (2.36%) that yields a ratio exactly equal to 1. This fact means that the bound K_{cr} is a good bound and cannot be decreased without decreasing the probability of reaching cohesiveness. Conversely, although the adopted implementation of the iterative scheme for K_{min} leads to a sort of quantization, this plot suggests a trade-off on how much the value of K can be decreased to ensure a minimum probability of cohesiveness. In particular, it can be stated that by decreasing K tenfold, phase cohesiveness in $\overline{\Delta}(\gamma_{min})$ can be obtained with a probability of about 60%.

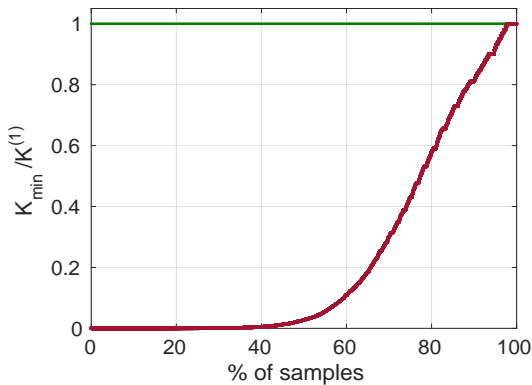


Fig. 4. Distribution of $K_{min}/K^{(1)}$: $K^{(1)} = K_{cr}/\sin(\gamma_{min})$ with K_{cr} obtained by (4); K_{min} is the value calculated through the iterative scheme.

Finally, it is possible to calculate the empirical probabilities of frequency synchronization obtained with $K = K^{(1)}$ and with $K = K_{min}$, which result in:

$$\widehat{P}_{fr, K^{(1)}} = 88.5\% \quad \widehat{P}_{fr, K_{min}} = 99.93\%.$$

By comparison with (15), it can be noticed that the value of $\widehat{P}_{fr, K^{(1)}}$ is perfectly in line with that of \widehat{P}_{fr} (taking into account the different set of Monte Carlo realizations), while $\widehat{P}_{fr, K_{min}}$ is much higher: in all likelihood, this is due to the fact that a lower value of K , which anyway permits to achieve phase cohesiveness, allows to reduce possible numerical issues and thus has to be preferred when using a numerical solver.

V. CONCLUSIONS AND FUTURE WORKS

Motivated by applications in the biological field and by the study of power network dynamics, in this work a modified Kuramoto model is discussed, which takes into account also the spatial configuration of the coupled oscillator nodes through a distance-dependent kernel function.

In this framework, a critical bound is derived for the strength coupling among oscillators in order to achieve frequency synchronization and phase cohesiveness. This bound is validated in terms of correctness and accuracy by means of numerical simulations on a general spatial configuration, where the interacting agents are distributed on a spherical domain. Statistical figures are obtained that confirm the validity of the approach. A trade-off between the value of the coupling strength and the probability of convergence is suggested to relax the strength bound.

In addition, the interesting case of a configuration where two different populations of oscillators interact, characterized by different kernel parameters, is considered. In such a scenario, it is obtained an upper bound to $\Delta\omega_{sync}$, which represents the shift between the synchronization frequency reached with two kernels, $\tilde{\omega}_{sync}$, and the zero one obtained with the single kernel ($\omega_{sync} = 0$ if $\omega \in \mathbf{1}_{\frac{1}{N}}$).

Many issues remain interesting for future investigation, among which the study of different types of kernel function, that may depend also on the actual state of the system, or the exploitation of particular spatial configurations (such as lattices): both these aspects are related to how the spreading of local information is accomplished through the system. Indeed, some insight gained from specific applications would be beneficial in order to provide more realistic case studies and suggest how to exert control and improve its performance to achieve global synchronization and cohesiveness.

APPENDIX I

A. Proof of Prop. 1

Proof: To prove the positive invariance of $\overline{Arc}_N(\gamma)$, i.e. the phase cohesiveness in $\overline{Arc}_N(\gamma)$ for some $\gamma \in [0, \pi]$, the function $V : \mathbb{T}^N \rightarrow [0, \pi]$ is introduced as

$$V(\theta) = \max\{|\theta_i - \theta_j| \text{ s.t. } i, j \in \{1, \dots, N\}\}. \quad (16)$$

The arc containing all the initial phases $\theta_i(0)$ has a maximum and a minimum: be $I_{max}(\theta)$ and $I_{min}(\theta)$ the sets of indices of angles $\{\theta_1, \dots, \theta_N\}$ equal to the maximum and the minimum, respectively. It follows:

$$V(\theta) = |\theta_{m'} - \theta_{l'}|, \quad \forall m' \in I_{max}(\theta), \quad \forall l' \in I_{min}(\theta). \quad (17)$$

Assuming $\theta_i(0) \in \overline{Arc}_N(\gamma)$, it is now to show that this condition remains $\forall t > 0$, which can happen if and only if $V(\theta) \leq \gamma \leq \pi$. It follows that $\overline{Arc}_N(\gamma)$ is positively invariant if and only if $V(\theta)$ does not increase at any time t such that $V(\theta(t)) = \gamma$.

The upper Dini derivative of $V(\theta)$ is given by [4]:

$$V'_+(\theta) = \limsup_{h \rightarrow 0} \frac{V(\theta(t+h)) - V(\theta(t))}{h} = \dot{\theta}_m(t) - \dot{\theta}_l(t), \quad (18)$$

where $m \in I_{max}(\theta(t))$ and $l \in I_{min}(\theta(t))$ are such that $\dot{\theta}_m(t) = \max\{\dot{\theta}_{m'}(t) \mid m' \in I_{max}(\theta(t))\}$ and $\dot{\theta}_l(t) = \min\{\dot{\theta}_{l'}(t) \mid l' \in I_{min}(\theta(t))\}$; along the system dynamics (2), (18) can be written as follows:

$$V'_+(\theta) = \omega_m - \omega_l - \frac{K}{N} \sum_{i=1}^N W(m, i) \sin(\theta_m - \theta_i) + \frac{K}{N} \sum_{i=1}^N W(l, i) \sin(\theta_i - \theta_l), \quad (19)$$

where all phases θ 's are time-dependent, and this explicit dependence is henceforth omitted for simplicity of notation.

From $V(\theta) = \gamma$, it follows that $\theta_m - \theta_l = \gamma$ and

$$\begin{cases} \theta_m - \theta_i \in [0, \gamma] \subseteq [0, \pi] \Rightarrow \sin(\theta_m - \theta_i) \geq 0 \\ \theta_i - \theta_l \in [0, \gamma] \subseteq [0, \pi] \Rightarrow \sin(\theta_i - \theta_l) \geq 0 \end{cases} \quad (20)$$

Moreover the kernel property stands

$$W(i, j) \in [e^{-\tilde{\alpha}^2}, 1] \subseteq]0, 1], \quad \forall i, j \quad (21)$$

where $\tilde{\alpha} = \frac{\alpha_{max}}{p}$, which yields

$$V'_+(\theta) \leq \omega_m - \omega_l - \frac{K}{N} e^{-\tilde{\alpha}^2} \sum_{i=1}^N (\sin(\theta_m - \theta_i) + \sin(\theta_i - \theta_l)). \quad (22)$$

By means of prosthaphaeresis formulas applied to $\theta_m - \theta_i$ and $\theta_i - \theta_l$ the summation in (22) results

$$\sum_{i=1}^N 2 \sin\left(\frac{\theta_m - \theta_l}{2}\right) \cos\left(\frac{\theta_m - \theta_i}{2} - \frac{\theta_i - \theta_l}{2}\right) \quad (23)$$

and through the relations (20) it is:

$$\sin\left(\frac{\theta_m - \theta_l}{2}\right) = \sin\left(\frac{\gamma}{2}\right) \quad (24)$$

$$\cos\left(\frac{\theta_m - \theta_i}{2} - \frac{\theta_i - \theta_l}{2}\right) \geq \cos\left(\frac{\theta_m - \theta_l}{2}\right) = \cos\left(\frac{\gamma}{2}\right). \quad (25)$$

Going back to the derivative (22), it follows:

$$V'_+(\theta) \leq \omega_m - \omega_l - \frac{K}{N} e^{-\tilde{\alpha}^2} \sum_{i=1}^N 2 \sin\left(\frac{\gamma}{2}\right) \cos\left(\frac{\gamma}{2}\right) \quad (26)$$

$$\leq \omega_m - \omega_l - K e^{-\tilde{\alpha}^2} \sin(\gamma). \quad (27)$$

The length of the arc formed by the phases is non-increasing in $\overline{Arc}_N(\gamma)$ if for any pair $\{m, l\}$ it holds that

$$K e^{-\tilde{\alpha}^2} \sin(\gamma) \geq \Delta\omega \Rightarrow V'_+(\theta) \leq 0, \quad (28)$$

where $\Delta\omega = \max(\omega) - \min(\omega)$. For $\gamma \in [0, \pi]$, the left member of (28) is a concave function, whose maximum is at $\gamma^* = \pi/2$. Thus, there exists an open set of arc lengths $\gamma \in [0, \pi]$ satisfying (28) if and only if

$$K e^{-\tilde{\alpha}^2} > \Delta\omega, \quad (29)$$

which corresponds to the equivalent relations (4) and (5).

It follows that $\forall \gamma \in [\gamma_{min}, \gamma_{max}]$, $V(\theta)$ is non-increasing and it is strictly decreasing for $\gamma \in]\gamma_{min}, \gamma_{max}[$. As a consequence of that, the set $\overline{Arc}_N(\gamma)$ is positive invariant $\forall \gamma \in [\gamma_{min}, \gamma_{max}]$ and each trajectory starting in $Arc_N(\gamma_{max})$ approaches asymptotically $\overline{Arc}_N(\gamma_{min})$ (phase cohesiveness).

Furthermore, if (4) holds and hence (28) is true, there exists a unique $\gamma_{min} \in [0, \pi/2[$ and a $\gamma_{max} \in]\pi/2, \pi]$ which obey (28) with the equality sign:

$$\sin(\gamma_{min}) = \sin(\gamma_{max}) = \frac{1}{K} \frac{\Delta\omega}{e^{-\tilde{\alpha}^2}} = \frac{K_{cr}}{K}. \quad (30)$$

B. Proof of Prop. 2

Proof: From the Kuramoto model (2) written as

$$f_i(\theta) = \omega_i + \sum_{j=1}^N a_{ij} \sin(\theta_i - \theta_j), \quad (31)$$

with $a_{ij} = \frac{K}{N}W(i, j)$, it follows that

$$\frac{\partial f_i}{\partial \theta_i} = \sum_{j=1}^N a_{ij} \cos(\theta_i - \theta_j), \quad \frac{\partial f_i}{\partial \theta_j} = -a_{ij} \cos(\theta_i - \theta_j), \quad (32)$$

which implies that the Jacobian $J(\theta)$ satisfies

$$J(\theta) = -B \text{diag} \left(\{\tilde{a}_{ij}\}_{\{i,j\} \in \mathcal{E}} \right) B^T \quad (33)$$

where B is the incidence matrix of the graph \mathcal{G} with $\tilde{a}_{ij} = a_{ij} \cos(\theta_i - \theta_j) > 0$ since $|\theta_i - \theta_j| < \gamma_{min} < \pi/2$ for the phase cohesiveness. Moreover, $J(\theta)$ is negative semidefinite and equal to the graph Laplacian L_G . Hence, by differentiating the phase dynamics (2), the frequency dynamics is obtained as

$$\frac{d\dot{\theta}_i}{dt} = - \sum_{j=1}^N \tilde{a}_{ij}(t) (\dot{\theta}_i - \dot{\theta}_j) \quad i \in \{1, \dots, N\} \quad (34)$$

or equivalently

$$\frac{d\dot{\theta}}{dt} = -L_G(t) \dot{\theta}. \quad (35)$$

Since $\ker(L_G) = \text{span}(\mathbf{1}_N)$, it follows

$$\mathbf{1}_N^T \frac{d}{dt} \dot{\theta} = 0 \Rightarrow \sum_{i=1}^N \dot{\theta}_i(t) = \sum_{i=1}^N \omega_i = N\omega_{avg}. \quad (36)$$

The dynamics (35) can be regarded as a *linear consensus protocol* with time-varying strictly-positive weights and according to [4, Theorem 4.1] all frequencies $\dot{\theta}_i(t)$ synchronize exponentially:

$$\left\| \dot{\theta}(t) - \omega_{sync} \mathbf{1}_N \right\|_2 \leq \left\| \dot{\theta}(0) - \omega_{sync} \mathbf{1}_N \right\|_2 e^{-\lambda_{fs} t}, \quad (37)$$

with $\lambda_{fs} = \lambda_2(L_G) \cos(\gamma) \geq K e^{-\tilde{\alpha}^2} \cos(\gamma)$, where $\lambda_2(L_G)$ is the Fiedler value of L_G (Gershgorin disc Theorem). Therefore, if $K > K_{cr}$, exponential convergence of the frequencies $\dot{\theta}_i(t)$ to ω_{sync} is attained. ■

REFERENCES

- [1] J.A. Acebrón, L.L. Bonilla, C.J. Pérez Vicente, F. Ritort, and R. Spigler. The Kuramoto model: A simple paradigm for synchronization phenomena. *Rev. Mod. Phys.*, 77:137–185, Apr 2005.
- [2] M. Breakspear, S. Heitmann, and A. Daffertshofer. Generative models of cortical oscillations: neurobiological implications of the kuramoto model. *Frontiers in Human Neuroscience*, 4:art.190, 2010.
- [3] J. Cabral, E. Hugues, O. Sporns, and G. Deco. Role of local network oscillations in resting-state functional connectivity. *NeuroImage*, 57:130–139, 2011.
- [4] F. Dörfler and F. Bullo. On the critical coupling for kuramoto oscillators. *SIAM Journal on Applied Dynamical Systems*, 10(3):1070–1099, 2011.
- [5] F. Dörfler and F. Bullo. Synchronization in complex networks of phase oscillators: A survey. *Automatica*, 50(6):1539 – 1564, 2014.
- [6] F. Dörfler, M. Chertkov, and F. Bullo. Synchronization in complex oscillator networks and smart grids. *Proceedings of the National Academy of Sciences*, 110(6):2005–2010, 2013.
- [7] G. Dumas, M. Chavez, J. Nadel, and J. Martinerie. Anatomical connectivity influences both intra- and inter-brain synchronizations. *PLoS ONE*, 7(5):e36414, 05 2012.
- [8] S.R. Gois and M.A. Savi. An analysis of heart rhythm dynamics using a three-coupled oscillator model. *Chaos, Solitons & Fractals*, 41(5):2553 – 2565, 2009.
- [9] S. Gupta, A. Campa, and S. Ruffo. Kuramoto model of synchronization: Equilibrium and nonequilibrium aspects. *Journal of Statistical Mechanics: Theory and Experiment*, (8):R08001, 2014.
- [10] Y. Kuramoto. Self-entrainment of a population of coupled non-linear oscillators. In *International Symposium on Mathematical Problems in Theoretical Physics*, volume 39 of *Lecture Notes in Physics*, pages 420–422. Springer Berlin Heidelberg, 1975.
- [11] H. Mangesius, S. Hirche, and D. Obradovic. Quasi-stationarity of electric power grid dynamics based on a spatially embedded kuramoto model. In *American Control Conference (ACC)*, pages 2159–2164, June 2012.
- [12] M. Mesbahi and M. Egerstedt. *Graph theoretic methods in multi-agent networks*. Princeton series in applied mathematics. Princeton University Press, Princeton (N.J.), 2010.
- [13] D. Paley, N.E. Leonard, R. Sepulchre, D. Grünbaum, and J.K. Parrish. Oscillator models and collective motion: Spatial patterns in the dynamics of engineered and biological networks. *IEEE Control Systems Magazine*, 27(4):89–105, 2007.
- [14] C.W. Reynolds. Flocks, herds and schools: A distributed behavioral model. *SIGGRAPH Comput. Graph.*, 21(4):25–34, August 1987.
- [15] J.A.S. Scott Kelso, G. Dumas, and E. Tognoli. Outline of a general theory of behavior and brain coordination. *Neural Networks*, 2012.
- [16] S.H. Strogatz. From kuramoto to crawford: exploring the onset of synchronization in populations of coupled oscillators. *Physica D: Nonlinear Phenomena*, 143(14):1 – 20, 2000.
- [17] S.H. Strogatz. *Sync : the emerging science of spontaneous order*. Theia, New York, 2003.
- [18] A.T. Winfree. *The geometry of biological time*. Biomathematics. Springer Verlag, New York, 2 edition, 2001.